# ZIMPOL-3: a powerful solar polarimeter

Renzo Ramelli[a], Silvano Balemi[b], Michele Bianda[a], Ivan Defilippis[b], Luca Gamma[b], Stephan Hagenbuch[c], Marco Rogantini[b], Peter Steiner[c] and Jan O. Stenflo[a,c]

[a]Istituto Ricerche Solari Locarno, Via Patocchi, Locarno, Switzerland;
[b]Scuola Universitaria Professionale della Svizzera Italiana, Le Gerre, Manno, Switzerland
[c]Institute of Astronomy, ETH Zurich, Zurich, Switzerland

## ABSTRACT

The area of high precision solar spectropolarimetry has made great advances in recent years and the Zurich IMaging POLarimeter (ZIMPOL) systems have played a major role in that. ZIMPOL reaches a polarimetric accuracy of $10^{-5}$ by using fast (kHz) polarization modulation/demodulation of the light beam in combination with large-area array detectors. A new generation of improved cameras (ZIMPOL-3) are being implemented for the scientific observations at the solar observatory at Istituto Ricerche Solari Locarno. The new system is based on a flexible and compact modular design, which easily adapts to new applications. A faster electronics and new sensors with higher quantum efficency compared to the previous ZIMPOL versions, allow to achieve a better overall efficency. Future plans include observing campaigns at foremost large telescopes and the exploration of new technologies (e.g. CMOS).

**Keywords:** Instrumentation, Polarimeter, Solar Spectropolarimetry

## 1. INTRODUCTION

The high polarimetric sensitivity down to $10^{-5}$ reached by the Zurich IMaging POLarimeter (ZIMPOL) systems allowed in the past 15 years to open new insights on different phenomena occurring in the solar atmosphere. In particular it has been possible to explore in great detail the faint signatures of scattering polarization that can be observed mainly near the solar limb and its spectral dependence. The spectral distribution of the linear polarization near the solar limb originated by scattering in the solar atmosphere is richly structured and is commonly called Second Solar Spectrum.[1] The scattering polarization signatures in the spectral lines are modified by the presence of a magnetic field through the Hanle effect.[2] This allows to access to new diagnostic capabilities on the solar magnetism.[3] The Hanle effect signatures give the possibility to obtain information on the magnetic fields, that are tangled below the resolution limit, and to which the Zeeman effect based diagnostics is blind due to cancellation effects.[4] Currently, studies are being carried out at the Istituto Ricerche Solari Locarno (IRSOL) in order to look at the variablity of the small scale magnetic fields looking in particular at the relation with the solar cycle.[5,6] Many important scientific spectropolarimetric observations have been carried out with the ZIMPOL polarimeters. Among them we recall in particular the three volumes of the Atlas of the Second Solar Spectrum obtained by Gandorfer and covering the wavelength range from 3160 Å to 6995 Å.[7–9]

The high sensitivity of ZIMPOL is obtained thanks to the high modulation frequencies ($> 1$ kHz), at which it operates. These frequencies are larger than the typical frequencies present in the power spectrum of seeing oscillations. The ZIMPOL operation is based on the following principle: The polarization state of the incoming beam $\vec{S}$ is transformed into a periodic intensity variation $I(t)$ (Fig. 1) by a fast variable retarder (modulator) followed by a linear polarizer. A synchronous demodulation is carried out by a masked CCD, on which the pixel rows are exposed alternatively with a proper shifting of the electron charges.

Having the growing scientific interest in precise polarization measurements in mind, a large effort has been invested since the beginning for the development and improvement of the ZIMPOL systems. We summarize here the main steps of the evolution of the ZIMPOL cameras. The first generation of cameras (ZIMPOL-1),[11] which were used mainly from 1994 to 1998, had every second pixel row on the CCD masked. Each camera allowed to obtain the measurement of only one polarization component at once, e.g. $Q/I$, $U/I$ or $V/I$. A second generation of cameras, ZIMPOL-2, is available since 1998. In these cameras three out of each four pixel rows are masked. This allows to obtain simultaneously with one single camera the measurement of the full Stokes vector. In 2001

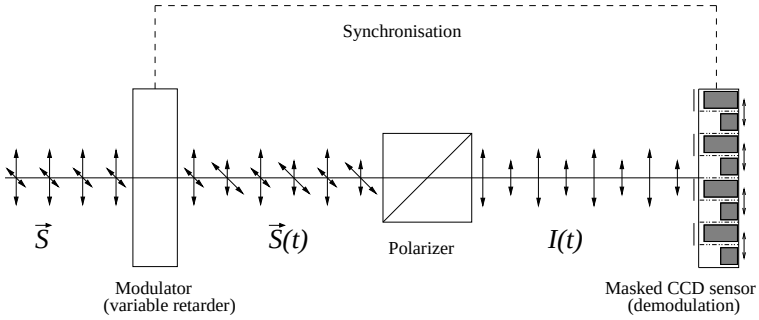


Figure 1. ZIMPOL principle.[10]

the CCD manufacturer was able to deliver masked front-side illuminated CCD's with an open electrode structure which are also sensitive to the UV.[12] The drawback in the loss of efficency because of masking, has been overcome end of 2006, with the successful installation of a cylindrical micro-lense array over the CCD surface, that focus the light on the open pixel rows. This allows an increase in the efficency of about a factor 4 (even up to a factor 6 in the UV region).

The last generation of cameras based on state of the art electronic components, are being implemented for the scientific observations at the solar observatory at IRSOL[13] and represent the core of the new ZIMPOL-3 system. The new system is very flexible and allows configurations for a wide range of polarimetric applications in astronomy. Some of the new features of ZIMPOL-3 compared to ZIMPOL-2 are:

- **Flexible and compact system**: The camera electronics, and acquisition control are included in the camera head.
- **Faster readout speed**: Parallel redout and integrating is possible after shifting the charges on the covered half of the detector
- **Adaptable to different CCD chips**
- **Based on newer technology**: replace components are available on the market
- **More functions**: different readout modes are available: binning, sub-frame readout, different demodulation schemes, electronic compensation of telescope polarization offset

## 2. THE ZIMPOL SETUP

Present and past versions of ZIMPOL can be considered as a modular system. The key components are the modulator and the special CCD camera which is able to synchronously perform the demodulation. The high modulation rate (in the kHz regime), which is larger than the frequency range of seeing, allows to get rid of seeing induced cross talk. Another advantage of the system is that the same physical pixels are used for each differential polarization measurement so that the system is free from gain table noise effects typical of a dual beam polarimeter. As a result the polarimetric precision is mainly limited by photon statistics down to the order of $10^{-5}$.

The system can be easily transported and adapted to different telescopes. Several successful observing campaigns have been organized with the ZIMPOL-1 and -2 versions at different foremost telescopes worldwide (McMath-Pierce telescope, Thémis, Swedish Solar Telescope, Dunn Solar Telescope). We plan to do the same with the new ZIMPOL-3 version. It is planned to install it also at the new Gregor Telescope in Tenerife.

The block diagram on Fig. 2 shows the current usual observing setup for the ZIMPOL-3 system at Istituto Ricerche Solari Locarno (IRSOL), which can be considered as the homebase of the system. Before to reach the ZIMPOL-3 camera, the light beam crosses different components:

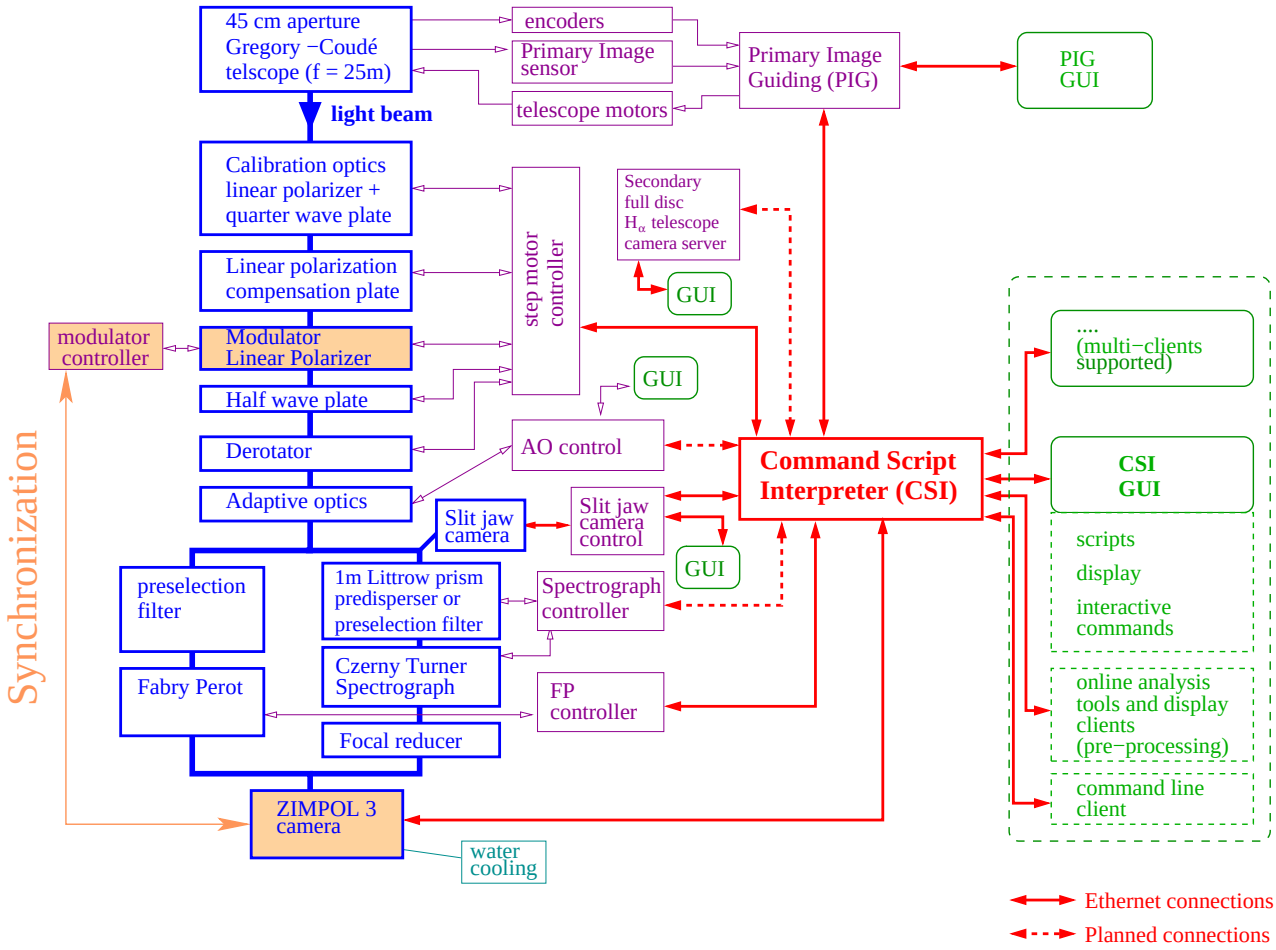


Figure 2. Block diagram showing the observing setup with the ZIMPOL-3 system at IRSOL. Represented are the optical components crossed by the beam (thick rectangles on the left), the control units, the Ethernet connections, the central controlling software (CSI) and the user interfaces.

**Telescope** The 45 cm aperture Gregory-Coudé telescope has an effective focal length of 25 meters. The position can be controlled automatically by the *Primary image guiding* system (PIG).[14,15]

**Calibration optics** The calibration optics, which consists of a Glan-Thompson linear polarizer and an achromatic quarter wave plate, can be inserted and rotated in order to produce any kind of elliptical polarization. It is of advantage to place the calibration optics before any optical component generating remarkable amounts of instrumental polarization (e.g. folding mirrors). In the case of IRSOL setup, the calibration units is placed just after the exit window of the telescope. The instrumental polarization resulting from the two folding mirrors present inside the telescope is basically a function of declination only, and cancels out on the celestial equator. Thus it stay almost constant during one observing day and it is easy to compensate for or to take it into account in the data reduction,[16,17] also on the basis of specific measurements of the telescope Muller matrix.

**Compensation plate** A compensation plate whose orientation is controlled by two step motors, can be used in order to cancel out the linear instrumental polarization. This allows to reduce at the minimum the influence of the detector non-linearities that scale with the polarization offset. In future we plan to replace this optical compensation, acting on the programmable de-modulation times of the ZIMPOL camera. The basic idea

is to arrange the exposure time of each CCD pixel row, in order to obtain the most homogeneous illumination. This kind of compensation, which is still under development, will allow to compensate for the full Stokes vector.

**Modulator and linear polarizer** The modulator package (see section 3 for more details), which generates a time varying retardation, is followed by a linear polarizing cube. After the linear polarizer the polarization information is encoded into an intensity modulation.

**Half wave plate** A half wave plate is used to rotate the polarization plane, in order to maximize the reflection throughput of the spectrograph grating

**Derotator** A Dove prism derotator allow to obtain the desired orientation of the image on the focal plane and to compensate for the telescope image rotation.

**Adaptive optics** The *adaptive optics* (AO) system,[18] whose correction is based on a tip-tilt mirror and on a deformable mirror controlled by 37 actuators, can be optionally used in order to stabilize the image during the data taking. The AO control includes a limb tracking mode, which is of particular interest for scattering polarization measurements (Second Solar Spectrum) near the solar limb.

**The spectrograph and the Fabry Perot system** ZIMPOL is primarily suited for observations with the spectrograph, but it works as well in imaging mode with filtergraphs. At IRSOL the system is being operated in combination with

- **the Czerny-Turner echelle spectrograph** which has a 10 m focal length and is based on a 180 × 360 mm grating with 316 lines per mm and 63° Blaze angle. A 1 meter Littrow prism based predisperser or an interference prefilter is used to select the spectral band entering in the spectrograph and thus to avoid the overlap of different grating orders. Spectrograph observations at IRSOL are often obtained with a focal reducer (typical reduction factor of about 2). This allows to increase the luminosity per pixel and to cover a larger spectral window.
- **a Fabry-Perot filter system** based on two $LiNbO_3$ etalons.[19,20] This can also be used in a novel configuration in combination with the spectrograph.[21]

The different sub-systems are connected through the Ethernet to a central computer program called *Command Script Interpreter* (CSI) that coordinates the different tasks (see section 5). Different clients can connect to the CSI, including a specific Graphical User Interface (GUI). Different automatic procedures can be developed in form of a script.

## 3. THE MODULATION PACKAGE

A ZIMPOL system can be operated in principle with different kinds of fast modulators. Until now the following modulators have been successfully implemented:

- *Photoelastic modulators* (PEM)
- *Ferroelectric liquid crystal* (FLC) modulators

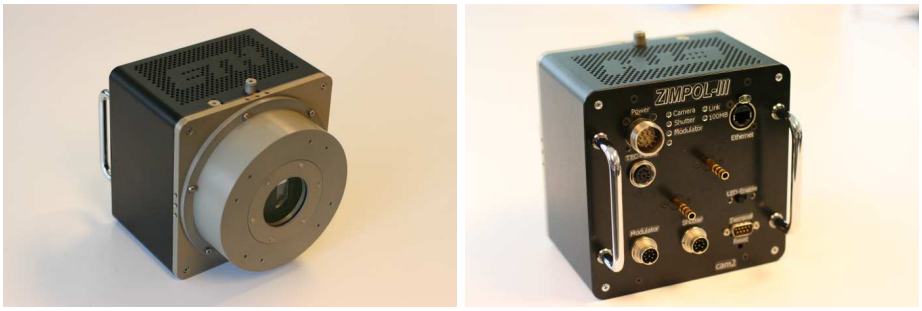


Figure 3. Front and back view of a ZIMPOL-3 camera.

### 3.1 Photoelastic modulator

Most of the ZIMPOL observations obtained at IRSOL were carried out with a PEM-90 model by Hinds with a useful aperture of 63 mm and a mechanical vibration eigenfrequency of 42 kHz. A detailed description of the modulator implemented in the ZIMPOL system is given by Gandorfer & Povel (1997).[22] PEMs have a good stability, optical quality and transmission. They can easily be tuned over a wide wavelength range including the UV.

One PEM generates a variable retardation with respect to a fix axis. Thus it is possible to obtain simultaneously the measurement of Stokes V and of the linear polarization component with respect to the PEM axis. To obtain the measurement of the other linear component the modulation package is mechanically rotated by 45 degrees*.

To record simultaneously all four Stokes components, one would need, in order to be compatible with the ZIMPOL demodulation principle, the usage of a pair of phase-locked PEM's in a configuration as proposed by Stenflo et al.(1992).[23] The setup includes (in order) a first PEM with the axis oriented at 45°, a second PEM at 0°, a quarter wave plate with the fast axis at 0° and a polarizer oriented at 22.5°. Unfortunately the attempts done in the past to synchronize two PEM's, each with its own eigenfrequency, did not achieve the required stability.

### 3.2 Ferroelectric liquid crystals

The synchronization of two FLC modulators is on the contrary straightforward since they operate with the modulation signal given by an external trigger. The modulation frequency is usually chosen to be 1 kHz. The ZIMPOL FLC package is composed by two FLC modulators intercalated by two zero-order retarder plates mounted in an aluminium-cylinder. The optimization of the orientation of the four optical components is described by Gisler (2005).[10] A thin layer of silicon oil between the optical surfaces strongly inhibits disturbing reflections. Thermo-electric elements stabilize the temperature.

## 4. THE ZIMPOL-3 CAMERA

The ZIMPOL-3 camera system (Fig. 3 and 4) is much more compact than in the previous ZIMPOL-2 version. With ZIMPOL-2 the camera electronics, and acquisition control consist of separate modules. In the ZIMPOL-3 system they are both included in the camera head. The connection with the users PC go through the local Ethernet. The other electronic connections to the camera consist of the power supply and the synchronization cable from the modulator. An optional RS232 connection is also available in case of need. A water circuit provides the secondary cooling.

Fig. 5 shows a high level block diagram of a ZIMPOL-3 Camera. A general description of each main block follows.

*The simultaneous measurement of the two linear polarization components is possible inserting a quarter wave plate before the modulator

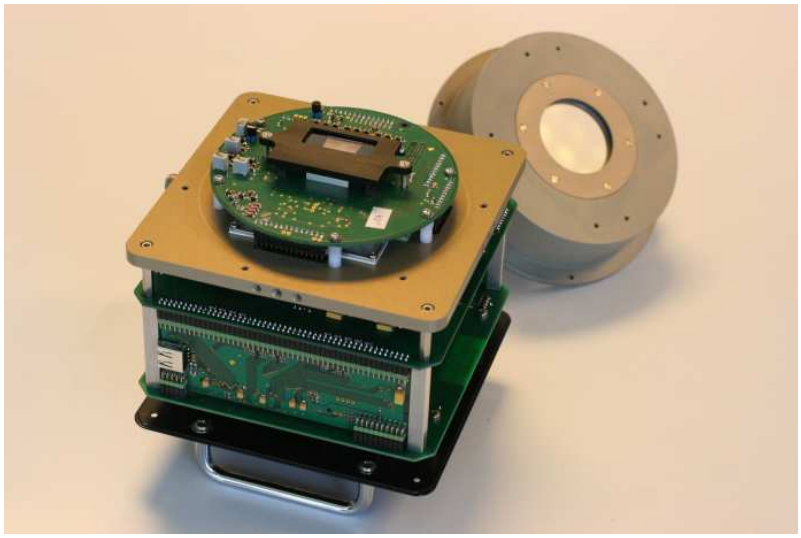

Figure 4. Internal electronics of the ZIMPOL-3 camera.

**XScale Computer Module** The camera contains a small embedded computer module made by Toradex (Colibri Module) running Linux v2.6. A server program accepts commands and sends data (acquired images) to an application host through Ethernet. The server implements high level camera functions and interacts with the rest of the camera hardware through a kernel device driver.

**Sync Logic** The main task of the *Sync Logic* block is to control an external modulator. This block, together with the *Acquisition Control* block are implemented in an Altera Cyclone FPGA. Two kind of modulators are supported: active and passive. The state of active modulators like FLC are driven by the Sync Logic block, i.e., the modulation frequency is generated by the block. On the other hand, passive modulators, like PEMs, modulate the light with an auto-resonant frequency. The Sync Logic block can in this case be programmed to synchronize the acquisition logic to this frequency. The camera supports frequencies up to 42 kHz (PEM modulation frequency).

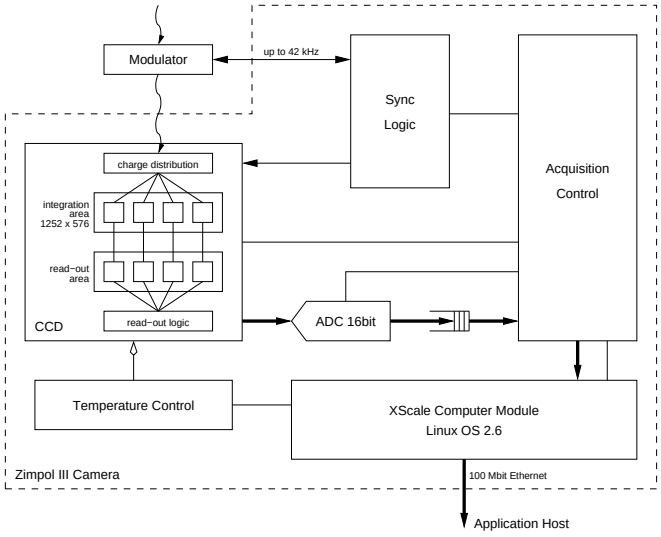


Figure 5. ZIMPOL-3 block diagram.

**CCD Interface** CCD sensor are plugged on substitutable *CCD Interface* boards. To install a new type of CCD sensor, just a new CCD Interface board is required, in addition to some software adjustments. Currently, the most used sensor is the CCD55-30 made by E2V. A board for the CCD55-20 sensors used by the ZIMPOL-2 cameras has also been built.

**Acquisition Control** The *Acquisition Control* block is in charge to do most of low level camera control functions: CCD, ADC, FIFO and Sync Logic are all controlled by this block. The block is in turn controlled from the software device driver in the Computer Module. Once CCD acquired data have made their way to the FIFO, the Acquisition Control block sends them to the Computer Module for subsequent TCP/IP encapsulation and Ethernet transmission. The system is designed to allow parallel readout (from the half covered CCD part) and integration (on the exposed half part of the CCD). The implementation of this functionality, which allows a significant decrease of the dead time, is in progress. Relatively slow paced control functions, such as vertical CCD charge movement for the demodulation, are handled by an assembly programmable *Timing Sequence Processor (TSP)*. The assembled TSP program is loaded by the Computer Module allowing the Acquisition Control block to support different demodulation schemas. Acting on the programmable shift times it is in principle possible to electronically compensate for the instrumental polarization, by adapting the exposure time of each demodulation step. This compensation procedure is still under development.

**Temperature Control** The CCD sensor is under vacuum and temperature control. The cooling can achieve -40°C below ambient temperature, the control process is software implemented in the Computer Module. The primary cooling is done by a Peltier thermoelectric device whose cold side is in thermal contact with the CCD, whereas the warm side is kept in thermal contact with a water cooling system.

### 4.1 The CCD sensors

As already mentioned ZIMPOL-3 can be adapted to different sensors. CCD55-30 backthinned sensors made by E2V with $2 \times 576(\mathrm{V}) \times 1252(\mathrm{H})$ pixels have been purchased and are currently used as main ZIMPOL-3 sensors. With respect to the sensors used with the ZIMPOL-2 system, they have a higher quantum efficency and a larger number of pixels. The new sensors have been equipped with a specific microlenses array (MLA) (Fig. 6). The MLA[†] consists of cylindric microlenses etched on a fused silicon substrate. On the back side of the substrate a stripe mask made of black chromium is structured to block stray light in three out of four pixel rows. The MLA is mounted with an active alignment process onto the CCD sensor. The masked side of the MLA is positioned very close to the CCD (about $10\mu$m). The distance is fixed by matched thin spacer.

## 5. SOFTWARE

ZIMPOL-3 is designed as a dynamically configurable distributed system. Any ZIMPOL-3 hardware units like a camera, a motor controller or other subsystems can be combined to a system basically by connecting them to the local Ethernet and by selecting some of these units from the software. The setup at IRSOL shown in Fig. 2 represents just one of the possible configurations. Each subsystem consists of a single chip or embedded processor, or a PC, depending on the hardware interface requirements. A ZIMPOL-3 server process running on this processor provides the specific functionality. In the normal operational mode, a Command Script Interpreter (CSI), realized in Java, mediate between user interfaces and functional subsystems. Its task is to serialize and break down complex commands into simple ones, coordinate concurrent actions, check their completion, store data, etc. Supported complex statements include calculations, conditionals, iterations, functions, procedures, parameter transformations, and sequential, parallel, background or unscheduled execution. Server based parameters can be referred like variables, although they may require communication. The interpreter is able to operate concurrently with multiple servers and multiple clients. The users can send commands through both scripts and interactive client entries (GUI or command line). To perform technical tests or for other practical reasons, a GUI may be also connected directly to a single functional unit.

[†]MLA and mounting are developed together with the Fraunhofer-Institut für Angewandte Optik und Feinmechanik (IOF) located in Jena, Germany

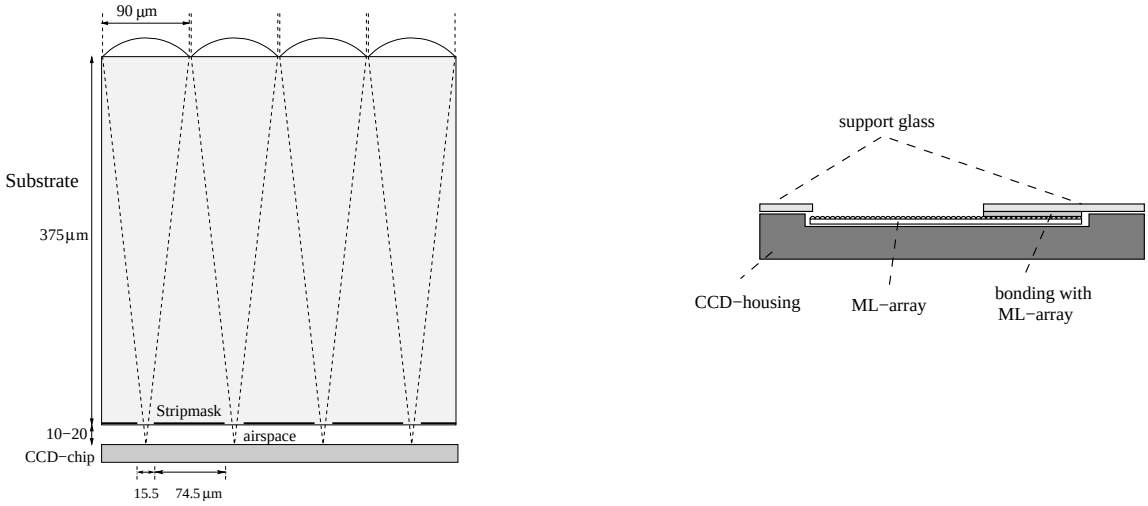


Figure 6. Left: Detail of the section of the cylindrical microlenses array mounted on the CCD55-30 sensor. Right: Microlenses array mounted on the CCD (schematic).

The units communicate through a unified type of symbolic duplex control streams over TCP/IP stream sockets. The general format of requests and replies is everywhere the same. It distinguishes parameters (that precede commands), commands, and status or exception messages. It is textual with one exception: large arrays (e.g. images) are included in binary format. Wherever appropriate, the units support parallel actions. A server may send an intermediate reply or progress message at any time.

The ZIMPOL-3 GUI is realized as a generic portable Java application whose layout, set of commands and parameters including their graphic representation can be determined by a simple descriptor file. All information about the command and parameter set of a subsystem is taken from an external textual definition file.

Interactive online analysis tool clients have also been developed. These allow to have an immediate look of the pre-reduced data in graphical formats or in form of statistic tables.

The offline data reduction and calibration follow basically the same procedures used for the ZIMPOL-2 system. We don't enter here into details and we refer to Gisler(2005)[10] and Gandorfer (2004)[12] for more details.

## 6. FIRST RESULTS

First spectropolarimetric observations made with the ZIMPOL-3 camera and the new CCD55-30 sensor in combination with the PEM look very promising. An example of Second Solar Spectrum observation and the corresponding profiles are shown on Figures 7 and 8. The profiles look compatible to the ones of Gandorfer Atlas,[7] but are much less noisy. The efficency improvement comparing our ZIMPOL-3 observation with Gandorfer's measurement, is clearly seen, also if one considers that his observations took at least 3 times longer and that he used a focal reducer giving a reduction factor of 3.15 while the optics present in our setup generates a reduction by a factor 1.86.

Note that when preparing the profiles shown on Figure 8, the polarization offset due to the $I \rightarrow Q$ crosstalk has been determined experimentally by assuming that it corresponds to the average value of polarization obtained in a flat-field observation, while in Gandorfer Atlas the offset has been chosen in order to have the same level of polarization in the continuum as the one expected according to the theory of Fluri and Stenflo (1999).[24]

We are presently alternating observations with the well known old ZIMPOL-2 system with the new ZIMPOL-3 system in order to check that they deliver compatible results. The agreement is generally very good.

In combination with strong absorption lines reaching almost complete absorption at line center, some spurious polarization signatures of few times $10^{-4}$ in term of fractional polarization may be seen (also in telluric lines where no signal is expected). This fact is currently under investigation. By rotating the camera by 180 degrees,

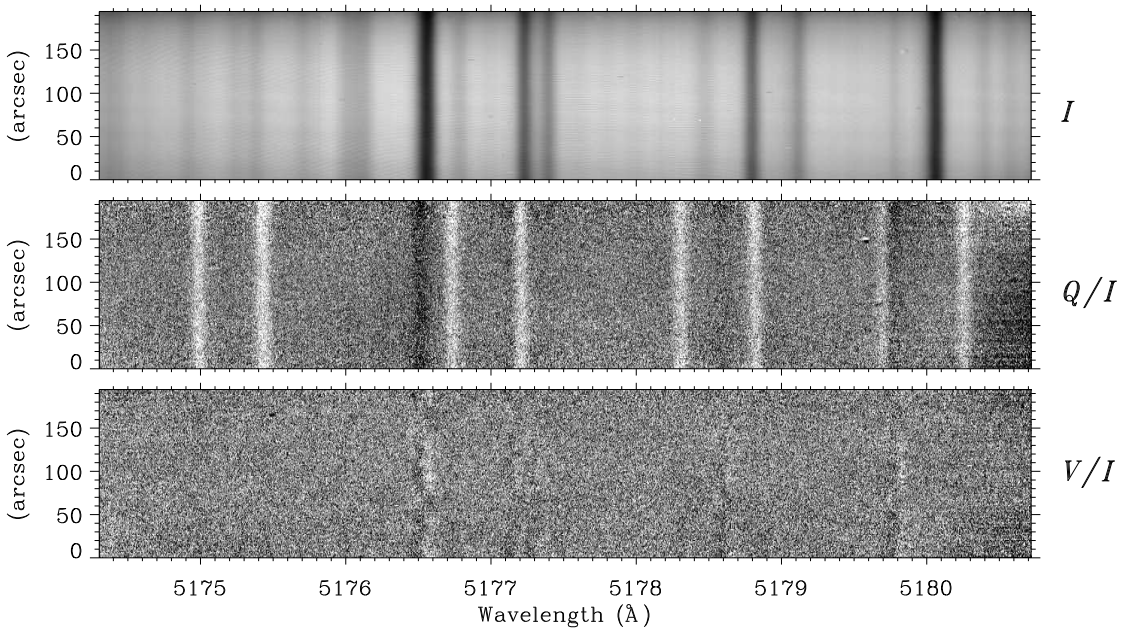


Figure 7. Example of observation obtained at the heliographic North Pole at about 12 arcsec inside the limb, with the masked CCD55-30 sensor mounted on a ZIMPOL-3 camera in combination with the PEM modulator. The observation consists of 500 frames of half second exposure time each. The Stokes $Q/I$ image shows the faint signatures typical of the Second Solar Spectrum. The corresponding profiles are reported on Fig. 8.

we could notice that the spurious signals stay constant with the beam and not with the camera reference system. Thus we could conclude that the problem is of optical nature and it is not due to the camera electronics or to the detector itself. The artifacts seem to be related with small vignetting of the light beam in the spectrograph optics, since we noticed that we could inhibit them by artifically reducing the telescope aperture with a mask in front of it. We suspect that vignetting in combination with a very tiny beam wobbling induced by the PEM is the cause of these small fake signals.

Compared with ZIMPOL-2, the new ZIMPOL-3 system is more efficient not only because it allows to use sensors with better quantum efficency, but also because of a smaller time overhead when taking data. Table 1 shows the overhead time comparison in the present situation, where the full potentialities of the ZIMPOL-3 system are not yet fully exploited. In fact we are still working on improving the data taking speed. As previously mentioned, we plan to implement the function that allows simultaneously integration and readout. In addition we are working on a more efficient pipelining of the data acquisition.

Table 1. Percentage of time lost for readout (overhead time) with respect to the total observing time when taking a large series of images with ZIMPOL-2 and ZIMPOL-3 in the present situation. Although the overhead is already now smaller for ZIMPOL-3 than for ZIMPOL-2, we plan to be able to further improve the overall ZIMPOL-3 readout speed in the near future

| Integration time per frame (seconds) | **ZIMPOL-2** CCD55-20 804 × 576 pixel (12 bits) | **ZIMPOL-3** CCD55-20 804 × 576 pixel (16 bits) | **ZIMPOL-3** CCD55-30 1280 × 576 pixel (16 bits) |
|---|---|---|---|
| 0.5 | 66% | 46% | 57% |
| 1 | 50% | 28% | 40% |

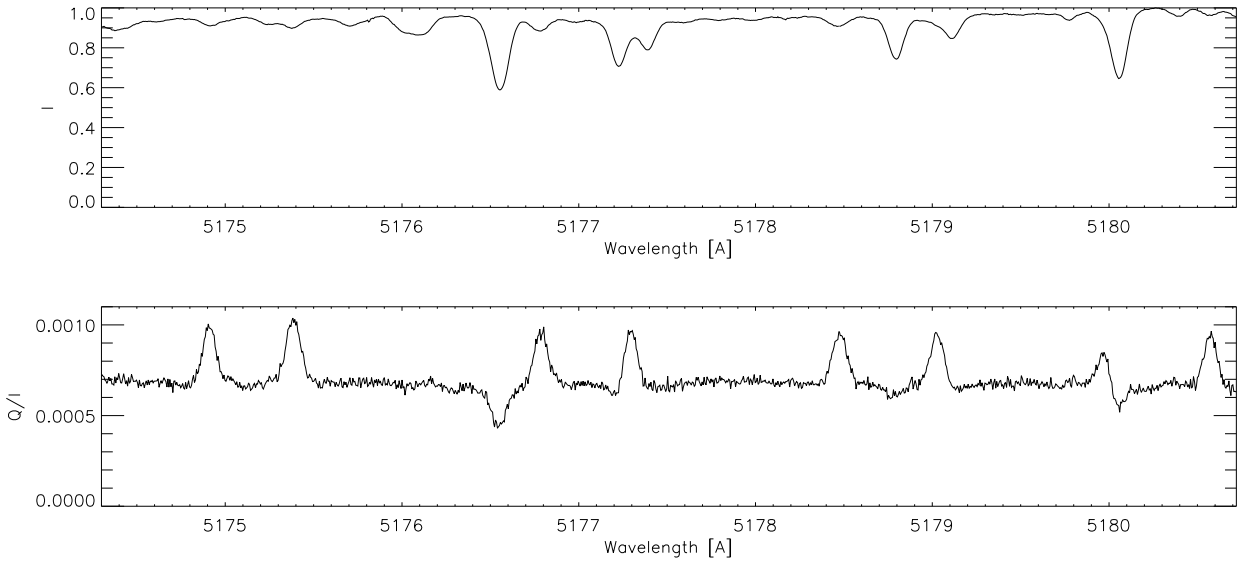


Figure 8. Scattering polarization profiles obtained from the observation reported on Fig. 7 after averaging along the spectrograph slit on the full observed spatial range. The 8 positive peaks in the linear polarization correspond to MgH, MgH, V, Fe, MgH, Ni, MgH, MgH. No smoothing has been applied.

## 7. CONCLUSION AND OUTLOOK

With the new ZIMPOL-3 system we could obtain results from first observations, that look very promising. The new system presents several advantages with respect to the old ZIMPOL-2 in terms of overall efficency, flexibility and compactness. We haven't yet exploited all potentialities of the new ZIMPOL-3 camera and we are still doing improvement and optimization works. In particular we plan to be able to further increase the system speed.

Once we will have gained sufficient experience with the new system, in order to demonstrate its reliability in comparison with the old ZIMPOL-2 system, we plan to completely replace ZIMPOL-2 with ZIMPOL-3 system in the all-days observations. We plan to use the new system not only at the IRSOL Gregory Coudé Telescope, but also at larger telescopes like Gregor and Thémis.

We think that the ZIMPOL technology could be very interesting also for the new large telescope projects as the Advanced Technology Solar Telescope (ATST) and the European Solar Telescope (EST).

For the future projects, however one should explore new evolution possibilities of the system, taking advantage of new technologies (like e.g. CMOS). In particular it would be very interesting to have a demodulating camera that get rids of the masking of the rows that is present in the current ZIMPOL versions.

## ACKNOWLEDGMENTS

The ZIMPOL-3 project started at Institute of Astronomy at ETH-Zurich in the group of Prof. Jan O. Stenflo. After the retirement of Prof. Stenflo the continuation of the project has been taken over by IRSOL and University of Applied Sciences of Southern Switzerland (SUPSI).

This project has been supported by Swiss National Science Foundation grant 200020-117821. IRSOL observatory is financed by Canton Ticino, ETHZ and City of Locarno together with the municipalities affiliated to CISL.

## REFERENCES


[1] Ivanov, V. V., "Analytical Methods of Line Formation Theory - are they Still Alive," in [*NATO ASIC Proc. 341: Stellar Atmospheres - Beyond Classical Models*], 81–+ (1991).

[2] Hanle, W., "Über magnetische Beeinflussung der Polarisation der Resonanzfluoreszenz," *Z. Phys.* **30**, 93–105 (1924).

[3] Berdyugina, S. V., Nagendra, K. N., and Ramelli, R., eds., [*Solar Polarization 5: In Honor of Jan Stenflo*], *Astronomical Society of the Pacific Conference Series* **405** (June 2009).

[4] Stenflo, J. O., "The Hanle effect and the diagnostics of turbulent magnetic fields in the solar atmosphere," *Solar Phys.* **80**, 209–226 (Oct. 1982).

[5] Bianda, M., Ramelli, R., and Stenflo, J. O., "Variation of the second solar spectrum with the solar cycle.," *Memorie della Societa Astronomica Italiana* **78**, 38–41 (2007).

[6] Kleint, L., Berdyugina, S., and Bianda, M., "Synoptic program - Variations of the Turbulent magnetic field," in [*12th European Solar Physics Meeting, Freiburg, Germany, held September, 8-12, 2008. Online at http://espm.kis.uni-freiburg.de/*], **12**, 2.71 (Sept. 2008).

[7] Gandorfer, A., [*The Second Solar Spectrum: A high spectral resolution polarimetric survey of scattering polarization at the solar limb in graphical representation. Volume I: 4625 Å to 6995 Å*], Zurich: VdF (2000).

[8] Gandorfer, A., [*The Second Solar Spectrum: A high spectral resolution polarimetric survey of scattering polarization at the solar limb in graphical representation. Volume II: 3910 Å to 4630 Å*], Zurich: VdF (2002).

[9] Gandorfer, A., [*The Second Solar Spectrum: A high spectral resolution polarimetric survey of scattering polarization at the solar limb in graphical representation. Volume III: 3160 Å to 3915 Å*], Zurich: VdF (June 2005).

[10] Gisler, D., *Instrumentierung für hochpräzise Vektorpolarimetrie in der Astronomie*, PhD thesis, ETH-Zurich (2005).

[11] Povel, H., "Imaging Stokes polarimetry with piezoelastic modulators and charge-coupled-device image sensors," *Optical Engineering* **34**, 1870–1878 (July 1995).

[12] Gandorfer, A. M., Steiner, P., Povel, H. P., Aebersold, F., Egger, U., Feller, A., Gisler, D., Hagenbuch, S., and Stenflo, J. O., "Solar polarimetry in the near UV with the Zurich Imaging Polarimeter ZIMPOL II," *Astron. Astrophys.* **422**, 703–708 (Aug. 2004).

[13] Bianda, M., Ramelli, R., and Gisler, D., "Observing the Second Solar Spectrum at IRSOL," in [*Solar Polarization 5: In Honor of Jan Stenflo*], S. V. Berdyugina, K. N. Nagendra, & R. Ramelli, ed., *Astronomical Society of the Pacific Conference Series* **405**, 17–21 (June 2009).

[14] Küveler, G., Wiehr, E., Thomas, D., Harzer, M., Bianda, M., Epple, A., Sütterlin, P., and Weisshaar, E., "Automatic guiding of the primary image of solar Gregory telescopes," *Solar Phys.* **182**, 247–255 (Sept. 1998).

[15] Küveler, G., Dao, V. D., Zuber, A., and Ramelli, R., "Robotic and Non-Robotic Control of Astrophysical Instruments," *Advances in Astronomy* **2010** (2010).

[16] Ramelli, R., Bianda, M., Trujillo Bueno, J., Merenda, L., and Stenflo, J. O., "Spectropolarimetric Observations of Prominences and Spicules, and Magnetic Field Diagnostics," in [*Chromospheric and Coronal Magnetic Fields*], D. E. Innes, A. Lagg, & S. K. Solanki, ed., *ESA Special Publication* **596** (Nov. 2005).

[17] Sanchez Almeida, J., Martinez Pillet, V., and Wittmann, A. D., "The instrumental polarization of a Gregory-coudé telescope," *Solar Phys.* **134**, 1–13 (July 1991).

[18] Ramelli, R., Bucher, R., Rossini, L., Bianda, M., and Balemi, S., "Adaptive optics system for the IRSOL solar observatory," in [*SPIE Conference Series*], **7736**, 131 (2010).

[19] Feller, A., Bianda, M., and Stenflo, J. O., "Imaging polarimetry with a tunable narrow-band filter," in [*Modern solar facilities - advanced solar science*], F. Kneer, K. G. Puschmann, & A. D. Wittmann, ed., 63–66 (2007).

[20] Feller, A., *Instrument Systems for Imaging Spectro-Polarimetry*, PhD thesis, ETH-Zurich (2007).

[21] Kleint, L., Feller, A., and Bianda, M., "Combination of two Fabry-Perot etalons and a grating spectrograph for imaging polarimetry of the Sun," *SPIE Conference Series* **7014**, 701414 (Aug. 2008).

[22] Gandorfer, A. M. and Povel, H. P., "First observations with a new imaging polarimeter," *Astron. Astrophys.* **328**, 381–389 (Dec. 1997).

[23] Stenflo, J. O., Keller, C. U., and Povel, H. P., "Demodulation of all four Stokes parameters with a single CCD - ZIMPOL II. Conceptual design.," *LEST Found., Tech. Rep.* **54** (1992).

[24] Fluri, D. M. and Stenflo, J. O., "Continuum polarization in the solar spectrum," *Astron. Astrophys.* **341**, 902–911 (Jan. 1999).